Processing and analysis of Hussar data for low frequency content

J. Helen Isaac, Gary F. Margrave, Monika Deviat*and Pam Nagarajappa*

ABSTRACT

Seismic data acquired by CREWES at an experimental low frequency shoot at Hussar, Alberta, in September 2011 were processed to attenuate unwanted noise and wavetrains and to retain or even enhance the low frequency content. We analyze the stacked data by creating plots of lateral phase-coherency versus frequency. The initial unprocessed data show strong coherency down to 7.5 Hz and weak coherency to 5 Hz but nothing below that.

The data processed by CREWES has radial filters and Gabor deconvolution applied for noise attenuation. The processed data show good coherency to 3 Hz but little in the range of 0-3 Hz. The same data processed by CGGVeritas had much more, and different, noise attenuation, resulting in coherency at the lowest frequencies of 1-5 Hz. Effective noise attenuation appears to be the greatest factor in attaining high coherency at these low frequencies.

We find that the phase-coherency plots are affected by processing procedures such as AGC and the amount of muting before stack. AGC adversely affects the coherency while the mute should not be so harsh as to remove desired frequency content. Geophone instrument response compensation, as far as we can tell at this time, does not enhance coherency at the lowest frequencies.

INTRODUCTION

In September, 2011, CREWES carried out an experimental low-frequency seismic shoot at Hussar, Alberta (Margrave et al, 2011). The line is 4.5 km long and runs NE-SW (Figure 1). There were many combinations of source types and receiver types but in this paper, we discuss the processing and analysis of the low dwell INOVA vibroseis data and the dynamite data, primarily recorded by 3C 10 Hz ARAM SM7 geophones, although we also show examples of data recorded by the Sunfull 4.5 Hz geophones. The vibroseis source was a custom-designed 1-100 Hz sweep that spent more time at the lowest frequencies than a regular linear sweep would do. The dynamite source was 2 kg at a depth of 15 m. The sources and the 4.5 Hz geophones were spaced 20 m apart and the 10 Hz geophones were spaced 10 m apart.

The data were processed by CREWES and by CGGVeritas to attenuate noise and enhance the low frequencies with the objective of producing data suitable for full waveform inversion. We analysed the data for its low frequency content by making phase-coherence plots that show reflection strength and continuity at the lowest frequencies.

*CGGVeritas

FIG. 1: Layout of the experimental low-frequency survey at Hussar.

DATA ANALYSIS

We performed preliminary phase-coherency analysis on all the data and presented the results in last year's CREWES report (Isaac and Margrave, 2011). This year we present phase-coherency analysis on data that were processed during the year. In this report, the data referred to as vibroseis is the custom low-dwell vibroseis data generated by the INOVA vibrator.

The phase-coherence analysis employed here is described in Margrave (1995; 1999) and is essentially a plot of f-x phase. In more detail, a space-time analysis window is selected and all traces falling in that window are Fourier transformed from time to frequency, giving the f-x spectrum. The temporal window applied to each trace is a boxcar with raised-cosine tapers applied at the beginning and end. The length of these tapers is set to roughly 20% of the window size but is allowed to fluctuate randomly from trace to trace. This disrupts any false coherence due to the window itself. The displays shown here are the sine and cosine of the f-x phase, plotted as consecutive samples for each frequency. Taking the sine or cosine of the phase removes any issues associated with phase wrapping. Then a simple wiggle-trace plot of the resulting f-x "phase" will show spatial coherence where signal is dominant and incoherence otherwise. In this paper we call such plots "phase-coherency plots". The algorithm has proven to be a reliable indication of signal content in normal frequency bands and we believe it is also reliable at very low frequencies. The algorithm is found in the CREWES Matlab library under the name "fxtran".

Figure 2 shows the phase-coherency plot (focussing on the 0-20 Hz bandwidth) of the unfiltered vibroseis data (a) and dynamite data (b) recorded by the 10 Hz 3C geophones. The parameters input to fxtran are an analysis window of 0.5–5.5 s, 20% taper and 20% random fluctuation. The only processing we applied to these data is a full-trace AGC to remove the effects of anomalous amplitudes, all statics and a custom-designed NMO stretch mute before stack. As indicated by lateral spatial continuity, the frequency content of both the vibroseis and dynamite is very good down to 7.5 Hz and some coherency is seen at 5 Hz, especially on the dynamite data. Below 5 Hz there is considerable noise. To study the effect of groundroll in the stacked data used for these phase-coherency plots, we applied surface wave noise attenuation to the shot gathers with a velocity of 375 m/s as the target. No further noise attenuation was applied at this time. Figure 3 shows the coherency plots for both the vibroseis and the dynamite data of the stacked groundroll (vibroseis: a, dynamite: b) and the data with this first pass of groundroll removal (vibroseis: c, dynamite: d). The groundroll manifests itself as non-linear events in the frequency range 0-5 Hz, which we term “noise”. Comparing Figures 2 and 3, we see that even a single pass of groundroll removal has removed some of the low frequency noise below 5 Hz, although further noise removal is still necessary.

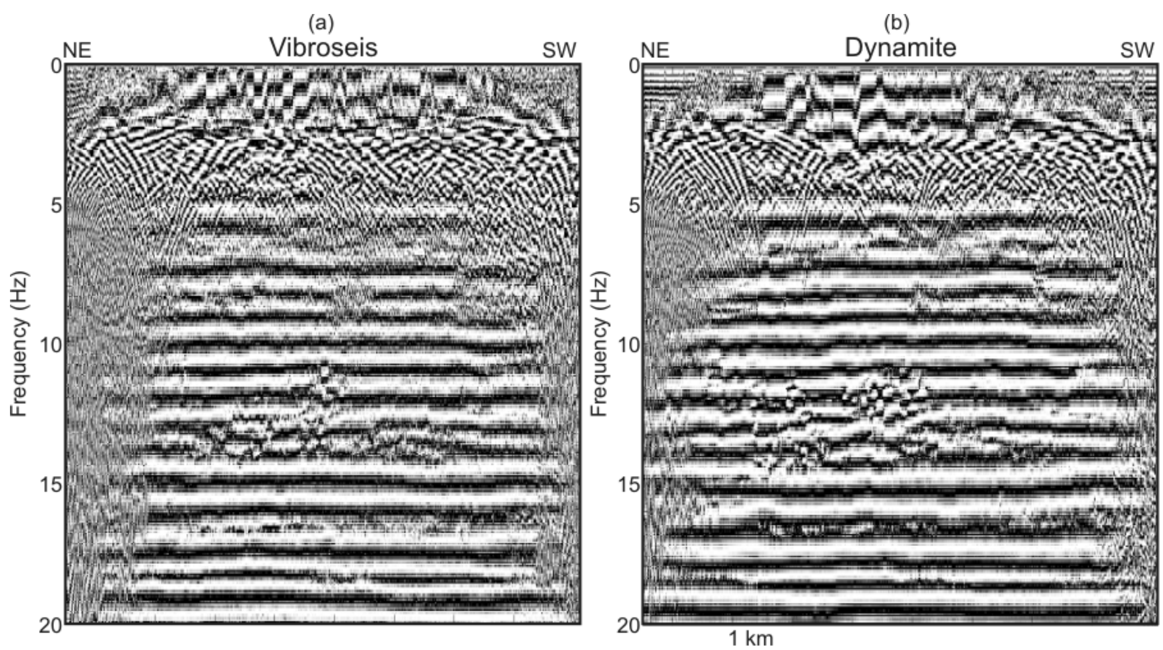

FIG. 2: Phase-coherency analysis of unfiltered stacked Vibroseis (a) and dynamite data (b) recorded by the 10 Hz geophones. We focus on the 0-20 Hz bandwidth. The only processing applied to the stacked data is a full-trace AGC, statics and NMO stretch mute.

CREWES processed the data with application of radial filters and Gabor deconvolution as the only forms of noise attenuation. Figure 4 shows the coherency stacks of the vibroseis (a) and dynamite (b) data with the radial filters applied. These radial filters were designed to target events with specific velocities that were not P-wave reflections. To see if we had truly removed undesired energy from the shot gathers, we subtracted the radial filtered data from the unfiltered data. The scaling and statics were identical for each shot gather. The results (Figure 5) show nicely the lack of coherence of the removed energy and the removal of the noise in the 2-5 Hz frequency band observed in Figure 2.

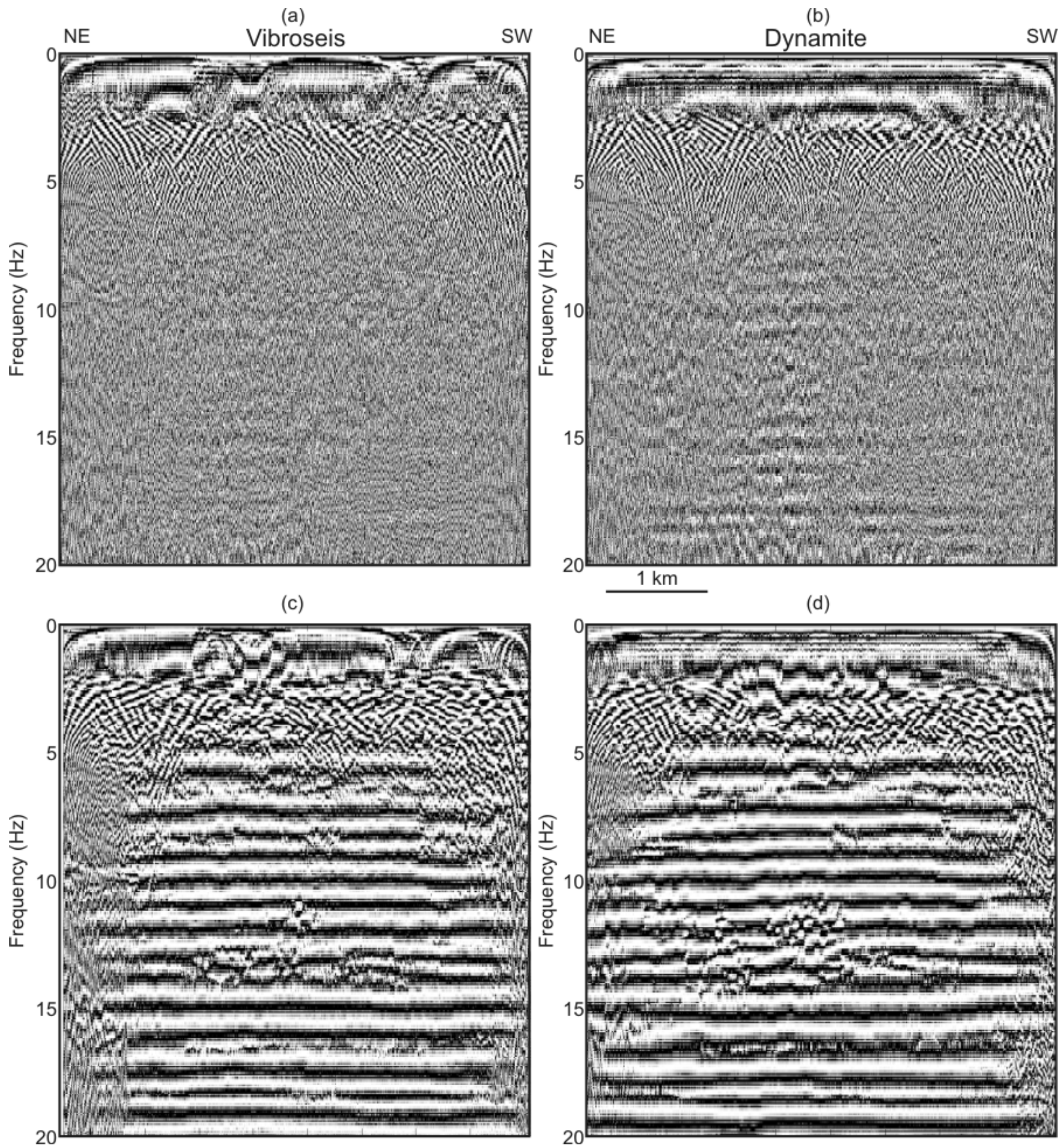

FIG. 3: Phase-coherency analysis of vibroseis data: stacked groundroll (a) and stacked data with this first pass of groundroll removal (c), and dynamite data: stacked groundroll (b) and stacked data with this first pass of groundroll removal (d).

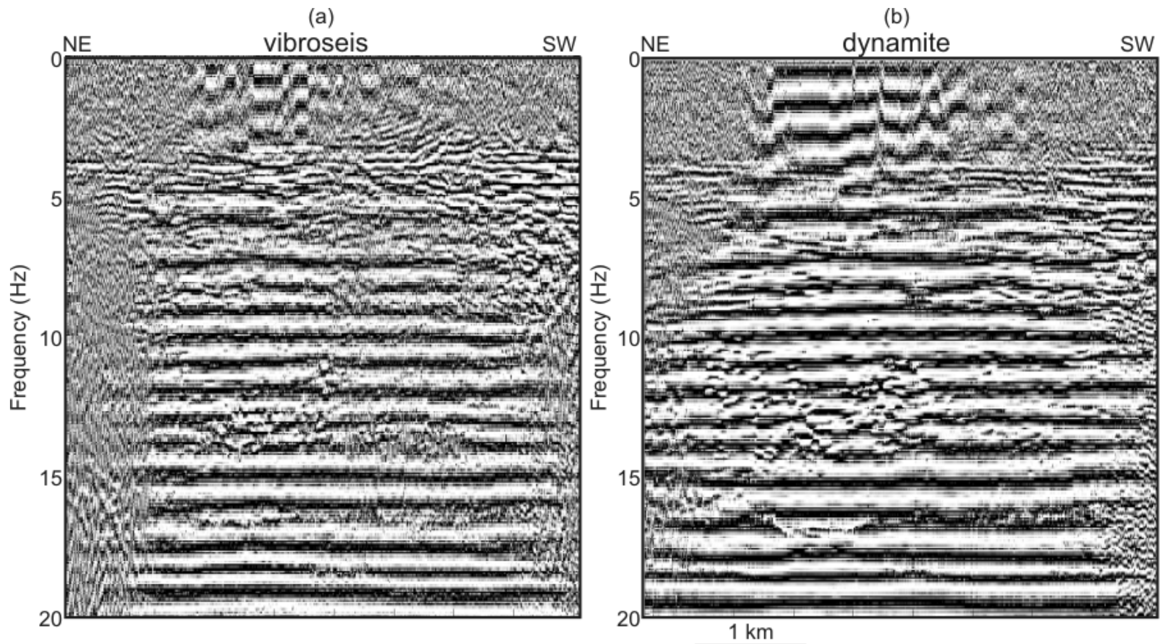

FIG. 4: Phase-coherency plots of stacked vibroseis (a) and dynamite (b) data with radial filters applied to remove undesired events. The data were recorded by the 10 Hz geophones.

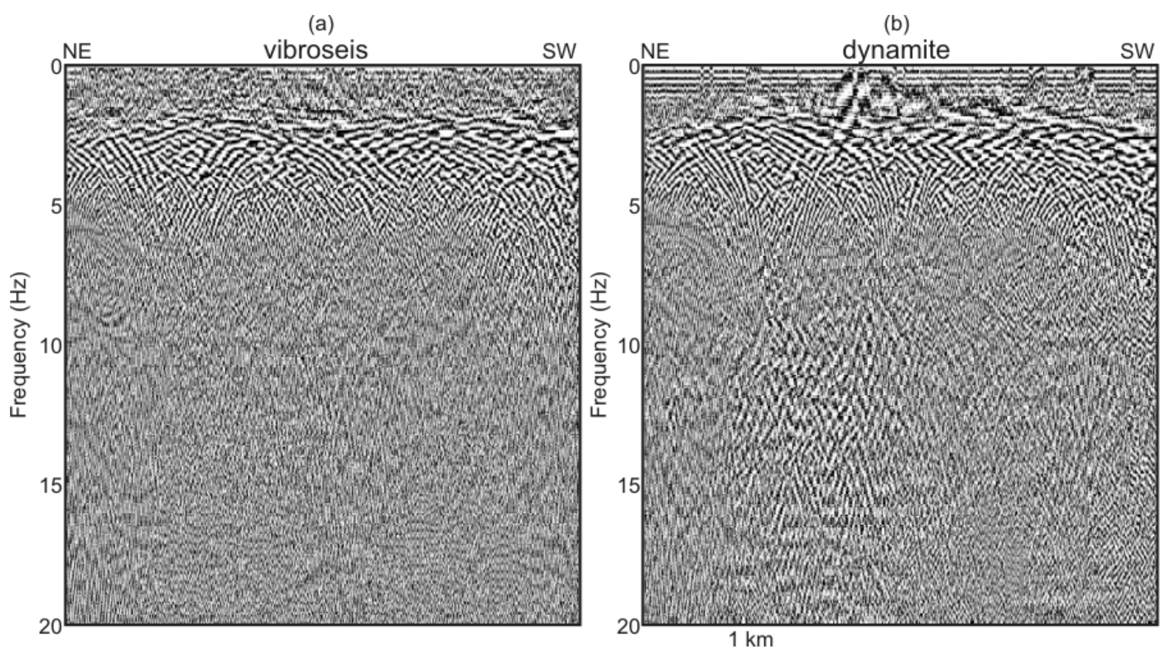

FIG. 5: Phase-coherency plots of stacked vibroseis (a) and dynamite (b) difference data. The datasets input to the stacks were the unfiltered shot gathers minus the radial filtered gathers, with identical statics and scaling. The data were recorded by the 10 Hz geophones.

In Figure 6 we show the coherency stacks of the data with the radial filters and Gabor deconvolution applied for the vibroseis (a) and dynamite (b) recorded by the 10 Hz geophones, vibroseis (c) and dynamite (d) recorded by the 4.5 Hz geophones, vibroseis (e) and dynamite (f) recorded by the Vectorseis accelerometers. After filtering the surface waves and other undesired wavetrains, the frequency content down to 5 Hz has been greatly improved and we might have frequencies to 3 Hz. An optimist might even detect frequencies below 3 Hz in the dynamite data. The type of receiver does not appear to make a significant difference towards the presence of low frequencies.

The dynamite data recorded by the 3C 10 Hz geophones were also processed by CGGVeritas, who made a greater effort than CREWES did to apply special noise attenuation techniques. CGGVeritas' noise attenuation included stationary sinusoid removal, several iterations of coherent noise attenuation, low and high frequency noise attenuation, high amplitude trace suppression and surface consistent scaling, either surface consistent deconvolution or Gabor deconvolution, and spectral balancing.

To observe how the data processing improved the resolution of the low frequencies, we analysed the stacked data at different stages of the CGGVeritas processing. In Figure 7a, the data had only sinusoid removal and gain recovery, while in Figure 7b coherent noise attenuation and high amplitude trace suppression were also applied. As expected before noise removal, the coherency at low frequencies is poor. We really only see coherent events down to 10 Hz, which is the resonant frequency of the geophones. Frequencies to 7.5 Hz appear faintly after the sinusoid removal. The application of surface consistent scaling and deconvolution (Figure 8a) does not make a significant improvement. Further noise attenuation after deconvolution (Figure 8b), however, does bring out coherent events in the very low frequencies although there is still noise between 7.5 and 3 Hz.

Further noise attenuation by scaling of low frequency, high amplitude noise and random noise attenuation using a semblance weighted dip filter results in much improvement (Figure 9a). Elimination of high frequency chatter (Figure 9b) does not make much difference to the plot in Figure 9a (but does improve the quality of the unshown stacked section).

The post-NMO mute has an effect on the coherency plot. For Figure 10 we applied two different mutes; one very harsh and the other not so harsh. The harsh mute has removed a lot of signal, which mute 2 leaves in to be stacked. The coherency of the stack with mute 2 is better at the 4-5 Hz frequencies.

Addition of a prestack short window length AGC harms the coherency (Figure 11). We are not quite sure why this happens but offer a suggestion that the AGC has boosted the amplitudes of residual noise, perhaps groundroll, in the data.

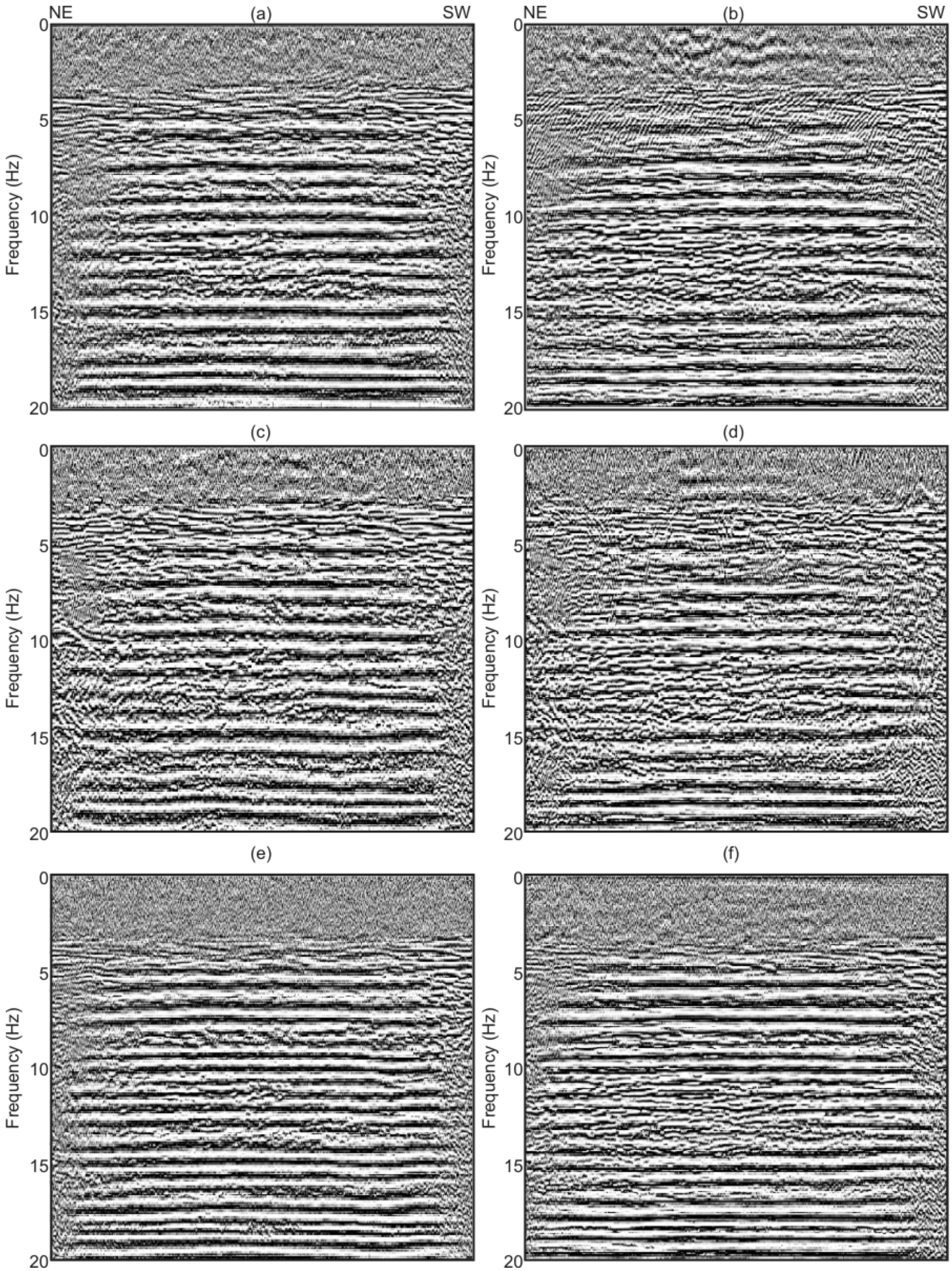

FIG. 6: Phase-coherency plots of stacked data with radial filters and Gabor deconvolution applied. The data were vibroseis (a) and dynamite (b) recorded by the SM7 10 Hz geophones; vibroseis (c) and dynamite (d) recorded by the Sunfull 4.5 Hz geophones and vibroseis (e) and dynamite (f) recorded by the Vectorseis accelerometers.

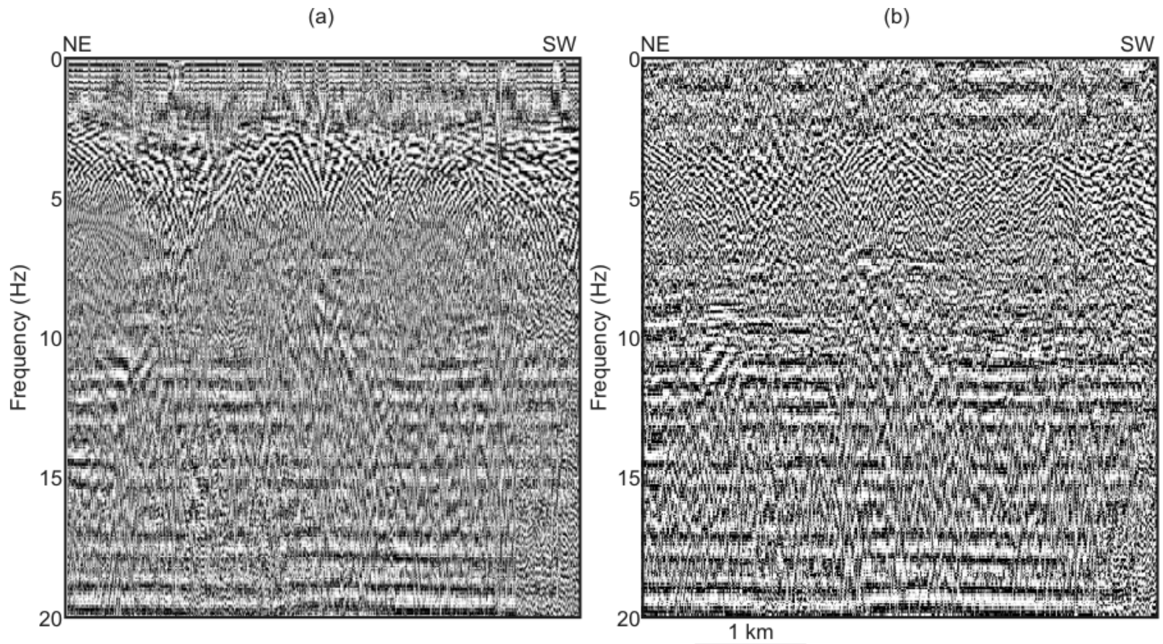

FIG. 7: Phase-coherency analysis of CGGVeritas-processed (a) stacked dynamite data with only sinusoid removal and gain recovery, and (b) stacked dynamite data with coherent noise attenuation and high amplitude trace suppression also applied.

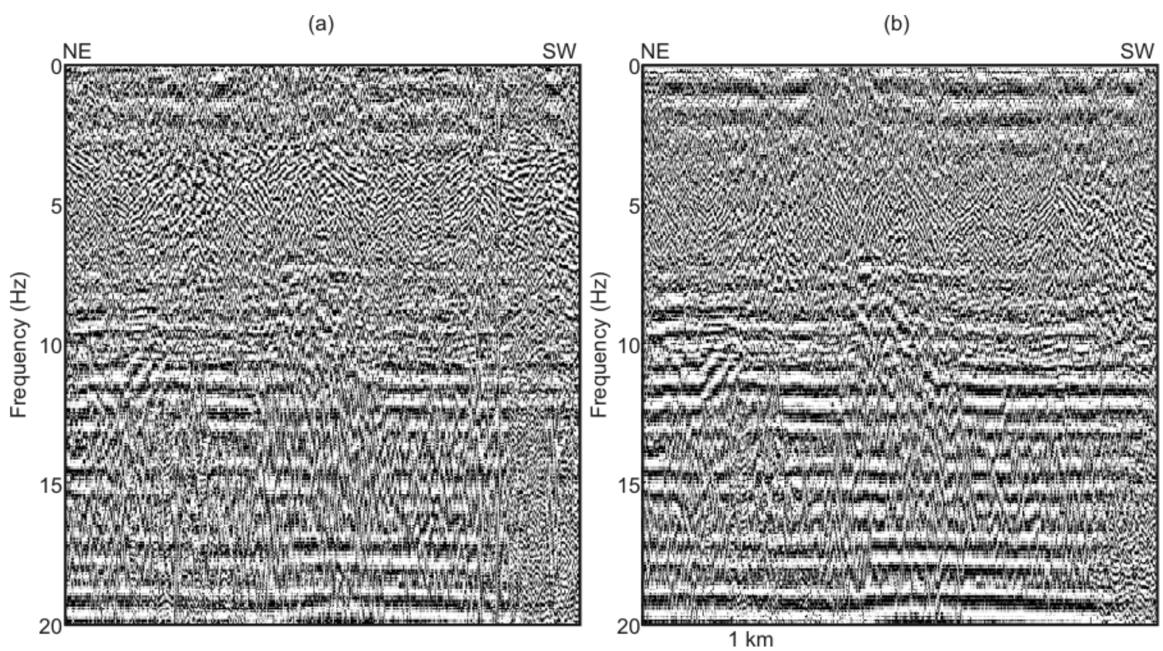

FIG. 8: Phase-coherency analysis of CGGVeritas-processed stacked dynamite data with (a) surface consistent deconvolution and (b) further coherent noise attenuation after deconvolution.

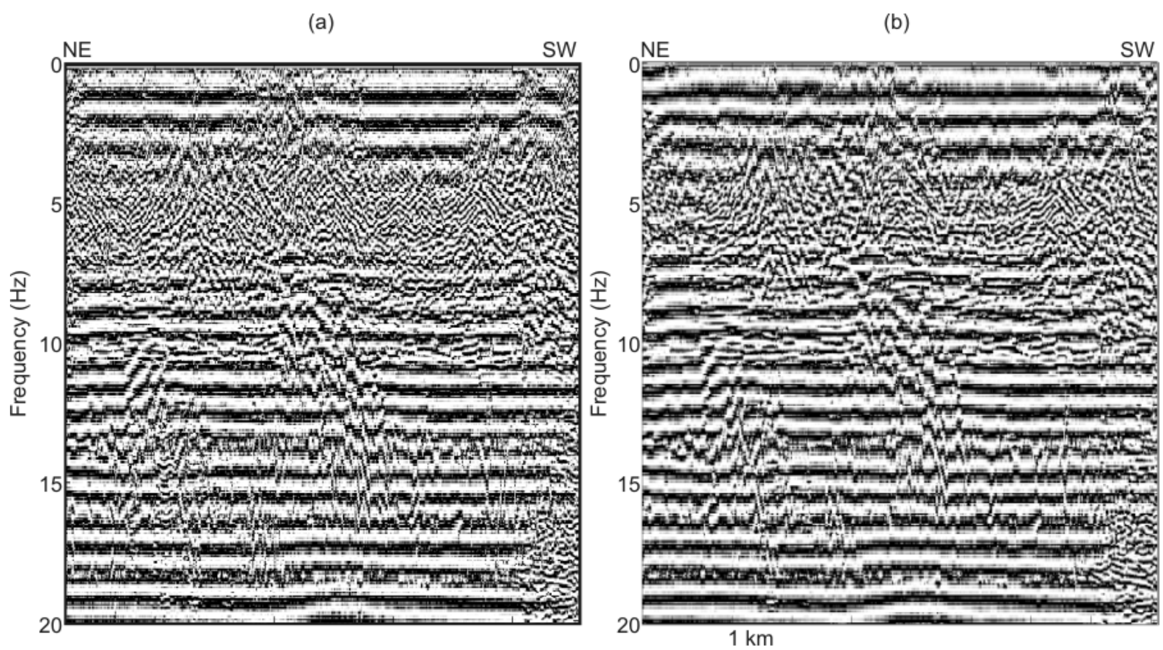

FIG 9: Coherency plots of CGGVeritas-processed stacked dynamite data after further noise attenuation (a) and some removal of high frequency chatter (b).

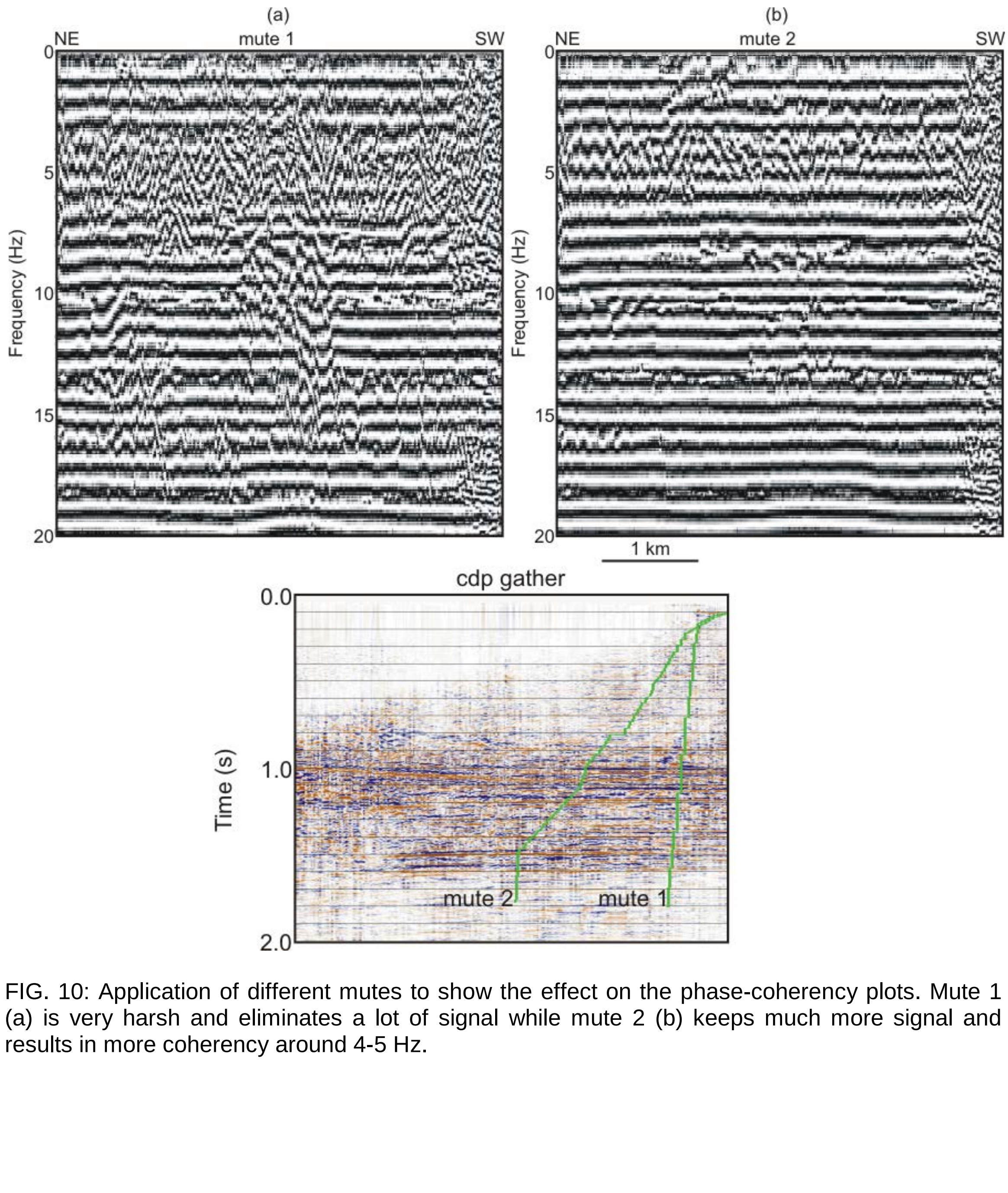

FIG. 10: Application of different mutes to show the effect on the phase-coherency plots. Mute 1 (a) is very harsh and eliminates a lot of signal while mute 2 (b) keeps much more signal and results in more coherency around 4-5 Hz.

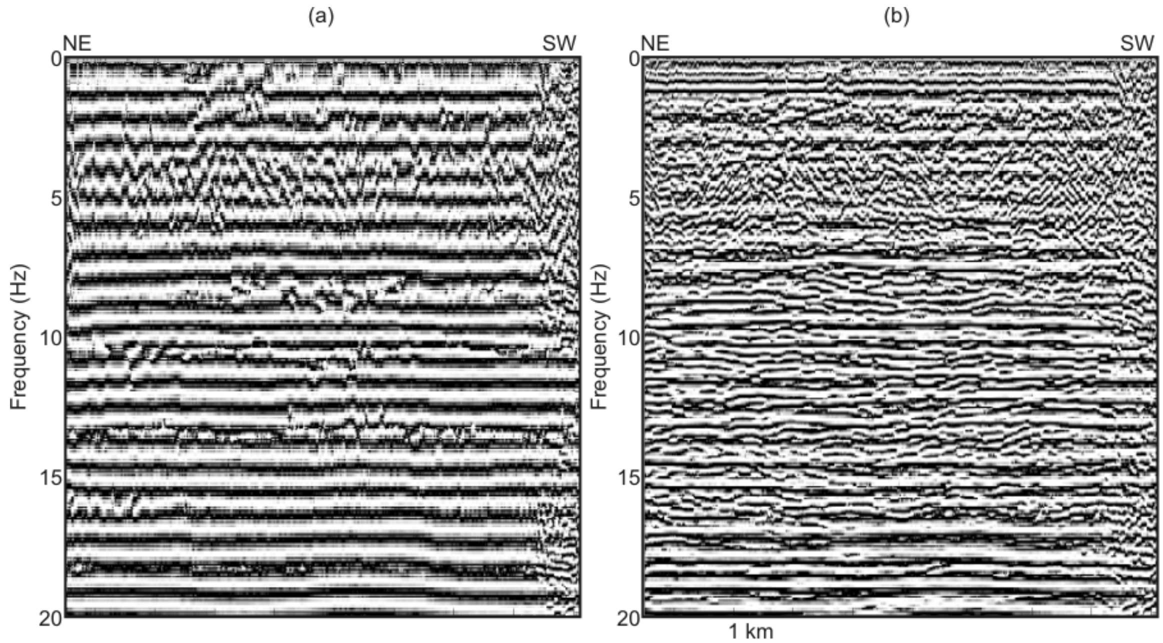

FIG. 11: Beware the evils of AGC. (b) shows the same dynamite data stacked in (a) but with the addition of a pre-stack short window length AGC, which has harmed the coherency.

CGGVeritas also processed a separate version of the dynamite data with geophone instrument response compensation applied. In Figure 12 we show comparisons of the data at an early stage of processing, before deconvolution, with and without the geophone instrument response compensation. The compensation appears to enhance slightly the coherency plots in the 2-6 Hz range but degrade them in the 6-10 Hz range. The compensated data was processed further in a similar manner to the first dataset but had a Gabor deconvolution applied rather than surface consistent spiking deconvolution.

Figure 13 shows phase-coherence analysis of the final stack for (a) the data with surface consistent deconvolution and (b) the data with geophone instrument response compensation and Gabor deconvolution. The data with geophone instrument response compensation and Gabor deconvolution appears to have more phase-coherency in the 5-7 Hz range but less in the 0-3 Hz range. It would be instructive to create a dataset with geophone instrument response compensation and surface consistent deconvolution to provide a better comparison of the compensated data with that of Figure 13a.

To show that our phase-coherency results are reproducible, in Figure 14 we show the phase-coherency plot generated by CGGVeritas of their stacked dynamite data. The analysis window was 0.5-4.9 s and the result is very similar to the phase-coherency we obtained over an analysis window of 0.5-5.5 s (Figure 13a).

For interest, we include a plot of the final migrated dynamite seismic section (Figure 15).

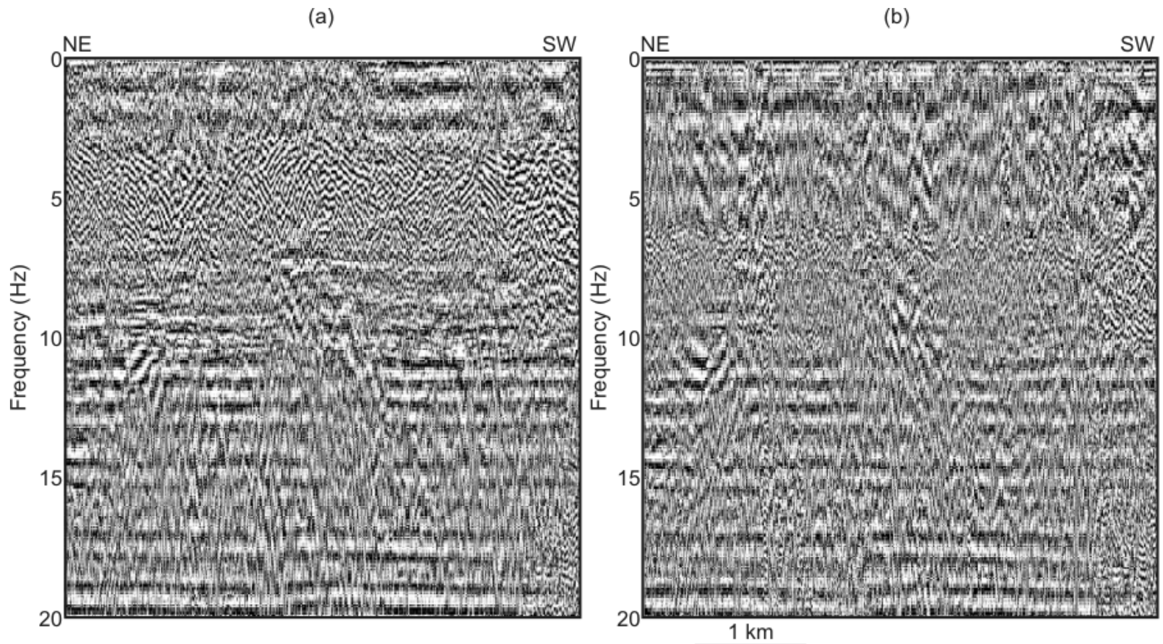

FIG. 12: Coherency plots of stacked dynamite data with some coherent noise attenuation and high amplitude trace suppression without (a) and with geophone instrument response compensation (b).

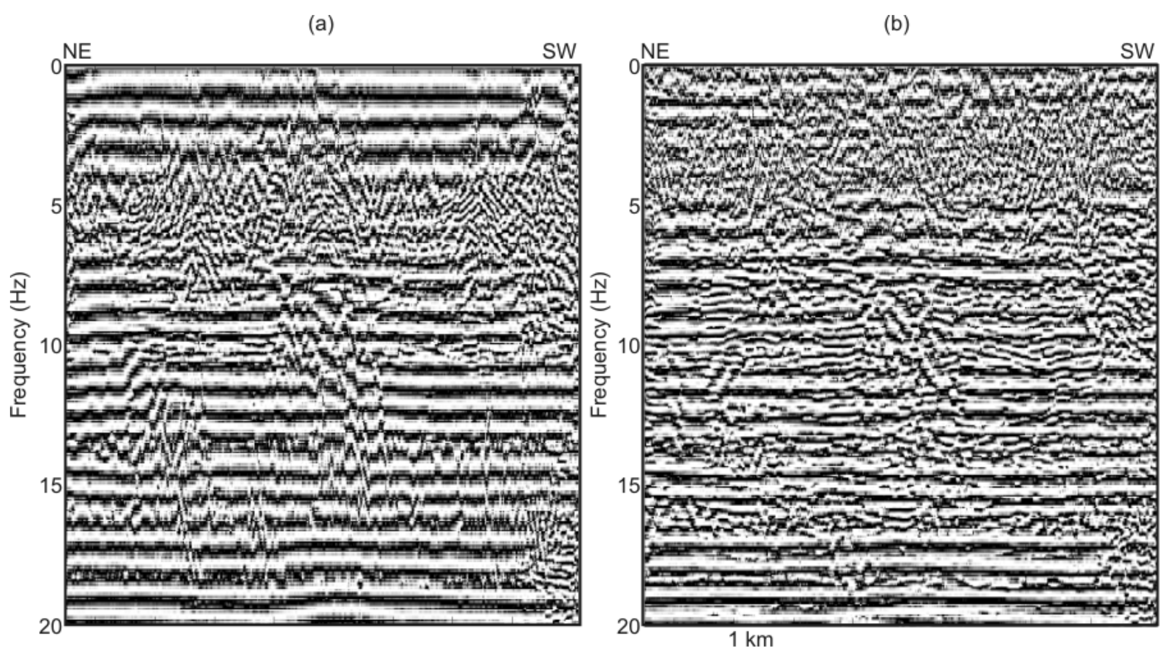

FIG. 13: Coherency plots of final stacked dynamite data with all noise attenuation and (a) surface consistent deconvolution and (b) geophone instrument response compensation and Gabor deconvolution.

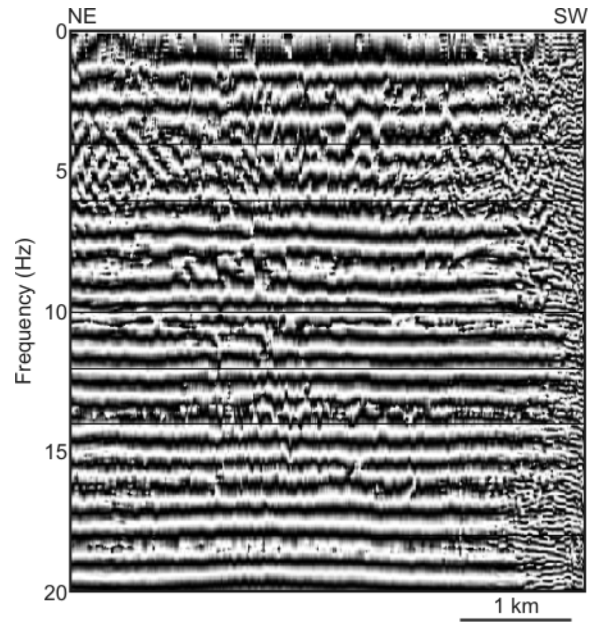

FIG. 14: Coherency plot created by CGGVeritas of the stacked processed dynamite data. The analysis window is 0.5-4.9 s.

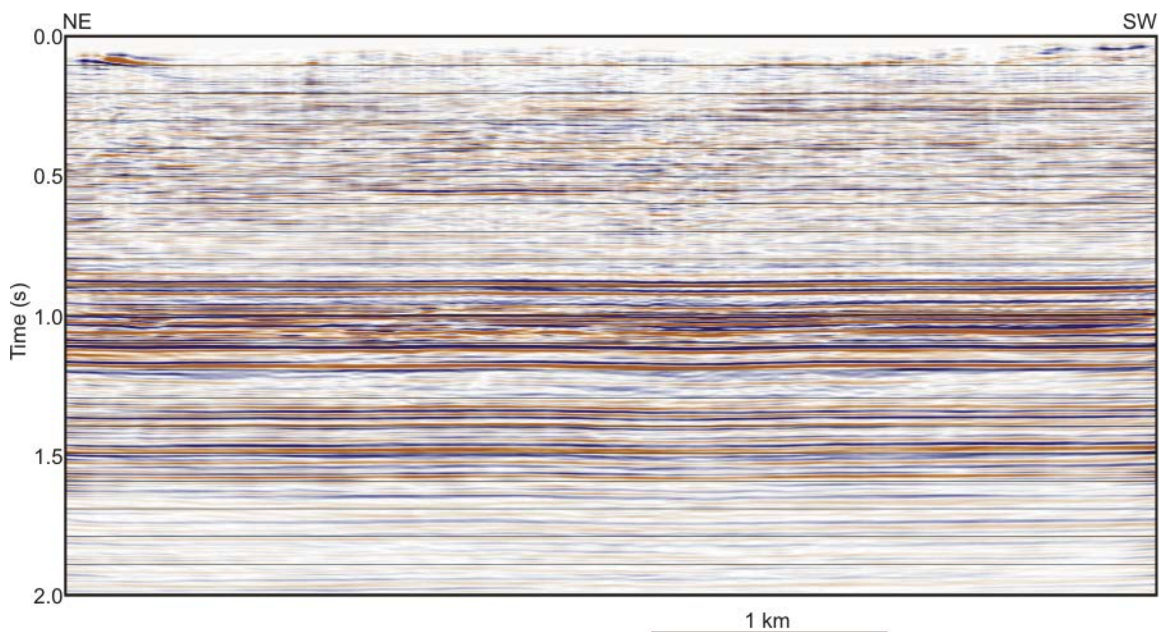

FIG. 15: Migrated dynamite data processed by CGGVeritas.

DISCUSSION

Seismic data with low frequencies (below 5 Hz) are necessary for full waveform inversion. Traditionally the lowest frequencies have been filtered out of the seismic data as they were considered to be undesirable and are present in unwanted groundroll. We are learning how to process seismic data to enhance the low frequency content while still attenuating the unwanted groundroll and other low frequency events in the data.

Phase-coherency analysis of seismic data from the experimental low frequency shoot at Hussar, Alberta, allows us to observe the frequency content of the data at different stages of data processing and thus to choose those processes that enhance the desired low frequencies and, perhaps more importantly, avoid those processes that degrade the desired low frequencies.

The initial unprocessed data show strong coherency down to 7.5 Hz and weak coherency to 5 Hz but nothing below that. After processing by CREWES with radial filters and Gabor deconvolution, the data show good coherency to 3 Hz but little in the range of 0-3 Hz. Stacks of the same dataset processed by CGGVeritas with much more noise attenuation display coherency at the lowest frequencies of 1-5 Hz. Efficient noise attenuation appears to be the greatest factor in attaining high coherency at the lowest frequencies. We appear to have phase-coherence, which is likely reflection signal, down to frequencies approaching 1 Hz in the Hussar data, especially with the dynamite source.

We find that the phase-coherency plots are affected by processing procedures such as AGC and the amount of muting before stack. Geophone instrument response compensation does not appear to enhance coherency at the lowest frequencies.

ACKNOWLEDGEMENTS

We thank the CREWES sponsors for their support and Landmark Graphics Corporation for ProMAX, with which CREWES did data processing. The phase-coherency plots were generated using Matlab. We thank CGGVeritas for processing the data and providing gathers and stacked data for this report.

REFERENCES

Isaac, J. H. and G. F. Margrave, 2011, Hurrah for Hussar! Comparisons of stacked data: CREWES Research Report vol. 23.

Margrave, G. F., 1995, Estimates of the signal band of the Blackfoot broad-band data: CREWES Research Report Vol. 7.

Margrave, G. F., 1999, Seismic signal band estimation by interpretation of f-x spectra: Geophysics, 64, 251-260.

Margrave, G. F., L. Mewhort, T. Phillips, M. Hall, M. B. Bertram, D. C. Lawton, K. Innanen, K. W. Hall and K. Bertram, 2011, The Hussar low-frequency experiment: CREWES Research Report Vol. 23.